PUBLISHED VERSION

James M. Bewes, Antony Morphett, F. Donald Pate, Maciej Henneberg, Andrew J. Low, Lars Kruse, Barry Craig, Aphrodite Hindson, Eleanor Adams
Imaging ancient and mummified specimens: dual-energy CT with effective atomic number imaging of two ancient Egyptian cat mummies
Journal of Archaeological Science: Reports, 2016; 8:173-177

© 2016 The Authors. Published by Elsevier Ltd. This is an open access article under the CC BY license (http://creativecommons.org/licenses/by/4.0/).

Originally published at:
http://doi.org/10.1016/j.jasrep.2016.06.009

PERMISSIONS
http://creativecommons.org/licenses/by/4.0/

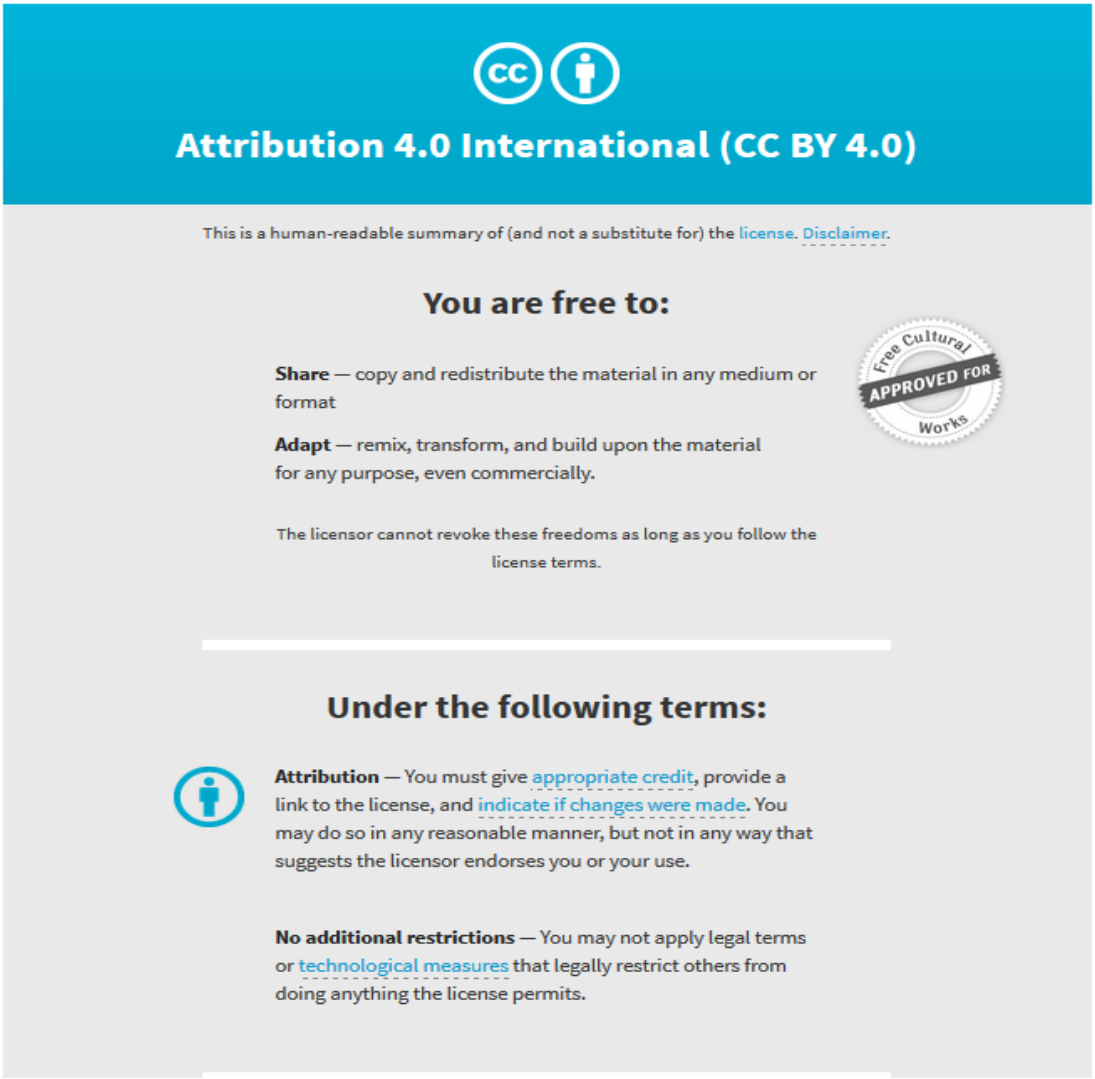

7 November 2017

http://hdl.handle.net/2440/108531

Journal of Archaeological Science: Reports 8 (2016) 173–177

Contents lists available at ScienceDirect

Journal of Archaeological Science: Reports

journal homepage: www.elsevier.com/locate/jasrep

Imaging ancient and mummified specimens: Dual-energy CT with effective atomic number imaging of two ancient Egyptian cat mummies

James M. Bewes [a,*], Antony Morphett [b], F. Donald Pate [c], Maciej Henneberg [d], Andrew J. Low [a], Lars Kruse [b], Barry Craig [e], Aphrodite Hindson [e], Eleanor Adams [e]

[a] Department of Radiology, Royal Adelaide Hospital, North Terrace, Adelaide 5000, Australia
[b] Dr Jones and Partners, Medical Imaging, 270 Wakefield St, Adelaide 5000, Australia
[c] Department of Archaeology, Flinders University, Adelaide, SA 5001, Australia
[d] Biological Anthropology and Comparative Anatomy Research Unit, School of Medical Sciences, University of Adelaide, Adelaide 5005, Australia
[e] South Australian Museum, Adelaide, SA 5000, Australia

ARTICLE INFO

Article history:
Received 8 April 2016
Received in revised form 3 June 2016
Accepted 3 June 2016
Available online 11 June 2016

Keywords:
Paleoradiology
Computed tomography
Ancient Egypt
Mummies
Paleopathology
Effective atomic number
Dual-energy CT
Animal mummies

ABSTRACT

In mummified animals and humans, soft tissues like skin and muscle become more dense over time due to dehydration. At the same time, bone becomes less dense as marrow is replaced by air. This is a problem for the radiological examination of ancient specimens, as currently used methods such as single-energy CT and MRI rely on density and water content to produce tissue contrast in an image. Dual energy CT with effective atomic number imaging overcomes this problem, as the elemental constituents and consequently effective atomic number of a specimen remain relatively constant over time. This case study of two ancient Egyptian cat mummies demonstrates that effective atomic number imaging can differentiate desiccated soft tissues from low-density bone in ancient remains. Effective atomic number imaging has the potential for superior tissue contrast resolution when compared to single energy CT and can be used to provide new paleoradiological perspectives.

© 2016 The Authors. Published by Elsevier Ltd. This is an open access article under the CC BY license (http://creativecommons.org/licenses/by/4.0/).

1. Introduction

1.1. Limitations of imaging ancient specimens using traditional single energy CT

A challenge in the field of paleoradiology, which is the radiological examination of ancient tissues, is differentiating between tissue types in mummified specimens. The combination of mummification processes and post-mortem changes cause the density of body constituents to become very similar. Bone becomes less dense as marrow is replaced by air, while soft tissues desiccate, becoming relatively more dense (Wanek et al., 2011). This presents a problem for the paleoradiologist, as conventional CT imaging depends heavily on a specimen's density to differentiate between tissue types (Bushberg and Boone, 2011; Gostner et al., 2013; Wade et al., 2012). This problem is magnified in small specimens, such as animal mummies, where spatial as well as contrast resolution is an issue.

Dual-energy CT offers a potential solution to the problem of converging material density in ancient specimens. By using two different x-ray energies to interrogate a material it is possible to derive a number of the material's properties that are unavailable on traditional, single energy CT scanners (Johnson et al., 2007; Wanek et al., 2011). Specifically, the electron density, effective atomic number and dual-energy index of a specimen can be calculated. These variables are potential discriminators between tissue types and inorganic materials for the paleoradiologist.

Effective atomic number imaging has theoretical advantages that make it a particularly promising candidate for use in paleoradiology. The effective atomic number of a specimen is independent of the density of a specimen (Brooks, 1977). While the density of ancient tissues changes over time, due to processes such as dehydration, the elemental constituents of mummified tissue stay relatively constant. Chemical variation due to tissue diagenesis is assumed to be comparatively small, particularly in specimens that are wrapped and not in direct contact with soil. Consequently, imaging with reference to atomic number should provide good discrimination between soft tissues and bone, as the latter has greater amounts of high atomic number elements such as calcium and phosphorus.

There are no published studies using atomic number imaging in the analysis of ancient remains. This preliminary study aims to demonstrate that dual-energy derived effective atomic number imaging is able to differentiate desiccated soft tissues from low density bone in ancient

* Corresponding author.
E-mail address: bewesj@gmail.com (J.M. Bewes).

http://dx.doi.org/10.1016/j.jasrep.2016.06.009
2352-409X/© 2016 The Authors. Published by Elsevier Ltd. This is an open access article under the CC BY license (http://creativecommons.org/licenses/by/4.0/).

remains and is a superior discriminator when compared to single energy CT.

If validated, atomic number imaging has the potential to improve paleoradiological diagnosis, enabling a better understanding of ancient pathologies and the cultures associated with them.

A secondary question that we aim to answer in analyzing the two cat mummies with imaging is regarding cause of death. It has been hypothesized that a common method of dispatching the cats prior to mummification was by cervical spine dislocation (breaking their necks) (Armitage and Clutton-Brock, 1981; Ikram, 2005). Consequently, a specific focus of the CT analysis is cervical spine integrity.

2. Materials and methods

2.1. Subject description and sample preparation

Two mummified ancient Egyptian cat specimens were made available by the South Australian Museum - specimen numbers A40436 and A40437 (Fig. 1). The specimens were acquired by the museum in the early 20th century however unfortunately little more is known regarding their provenance. Votive offerings in the form of animal mummies were associated with Egyptian cults celebrating living animal deities and became particularly popular from c. 600 BCE until the Roman era, ceasing at c. CE 250 (Ikram et al., 2015; McKnight et al., 2015). The cat mummies have not been previously imaged. Protective casings were removed for the study. One specimen was fixed to a wooden backing board, which was unable to be removed.

2.2. Dual energy imaging

Dual energy CT is well established in clinical radiological practice (McCollough et al., 2015) and a clinical scanner (SOMATOM Definition Dual Source; Siemens, Munich, Germany) was used. The samples were positioned perpendicular to the bore of the CT to reduce artifact. Samples were simultaneously imaged at 80 keV and 140 keV, as these energies are compatible with the post-processing software used to calculate effective atomic number maps. These energies also reflect the extremes of single-energy imaging on most CT scanners. Theoretically any two energy levels can be used to derive effective atomic number. Multiplanar reconstructions were performed at 0.75 mm intervals (matrix size 512 × 512). Imaging was performed at Dr. Jones and Partners, Calvary Wakefield Hospital, Adelaide on 17/12/2015.

Fig. 1. Mummified cats imaged in current study (A40436 and A40437).

2.3. Post-imaging data acquisition

Following image acquisition, post-hoc image analysis was performed using a commercially available software package (SyngoDE – Siemens) on a dedicated clinical radiology workstation. This software allows automated derivation of effective atomic number maps, as well as quantitative effective atomic number values within a user-designated region of interest (ROI).

2.4. Imaging and tissue analysis

Analysis and interpretation of the mummified cat bundles was performed by two radiologists using dedicated clinical radiology workstations with multiplanar reconstructions.

Different tissues types were identified in the scanned ancient remains and representative ROI markers placed on each tissue type. The ROI markers were necessarily very small in size, secondary to the small size of the mummified cats. Tissue types examined include cortical bone, trabecular bone, soft tissue and linen.

The tissue types were identified on conventional single-energy CT images by two radiologists using anatomical landmarks in regions of high intrinsic spatial and contrast resolution. For example, to obtain ROI's for cortical bone, long bones were identified and ROI's only placed on continuous cortical bone. ROI's were not placed where there was radiological ambiguity regarding the physical composition of a tissue on an anatomical basis, such as in conglomerate masses of tissue and bone within the central thorax or abdomen, or in areas of fragmented tissue and bone. Using unequivocal anatomical and morphological features to identify tissue types excluded regions of the specimens from analysis but was necessary to ensure the specificity of tissue ROI markers.

Within each ROI, the effective atomic number for the tissue type of interest was calculated. Hounsfield units (HU) at 80 keV and 140 keV were also recorded for comparison. At least 20 ROI's for each tissue type in each specimen were tabulated to obtain a representative sample. To improve the generalizability of the results, ROIs from both cat specimens were pooled for final analysis.

2.5. Statistical analysis

Derived imaging parameters were compared in a pairwise fashion to determine the imaging parameter that provides the best material contrast. Following a significant Kruskal-Wallis test, pairwise comparisons were made using non-parametric Mann–Whitney tests with Bonferroni adjustments made for multiple comparisons. (18 comparison groups used in total) An adjusted p-value of less than $0.05/18 = 0.003$ was used as significant. Statistical analysis was performed using a commercially available software package SPSS (IBM SPSS Statistics for Windows, Version 21.0).

Noting that effective atomic number imaging and traditional CT Hounsfield units use different scales, a derived non-parametric effect size estimate 'r' was obtained (Fritz et al., 2012) in order to measure contrast magnitude between the parameters under investigation. The higher the effect size, the greater the magnitude of contrast between two tissues. Using Cohen's effect size estimates, 0.1 is a small difference, 0.3 is a moderate difference and 0.5 is a large difference.

3. Results

3.1. Contents of mummified bundles: A40436 and A40437 imaging findings

Both specimens were confirmed to be feline. This was evidenced by the presence of feline dentition, appropriate thoraco-abdominal skeletal proportions and the presence of tails. Both specimens were skeletally mature and were positioned with forelegs projecting caudally, under body, and hindlegs and tail projecting cranially, also under the body. Multiple tissue types were identified within the specimen, including bone, soft tissue/skin conglomeration and wrappings.

In specimen A40436, the cervical spine was not identified in the neck and appeared displaced into the thorax. There were multiple disorganized bones scattered throughout the upper thorax. Multiple thoracic spinal fractures, a comminuted midshaft fracture of left hind leg femur and an oblique skull fracture were identified. No periosteal reaction or healing was evident in association with any of the fractures, suggesting the injuries were peri- or post-mortem.

In specimen A40437, multiple transverse cervical and thoracolumbar spinal fractures were identified. The fracture lines extend across the adjacent desiccated soft tissues, confirming these reflect post-mortem fracture lines (Fig. 2). There was a fracture of the right orbit. No periosteal reaction or healing was evident in association with any of the fractures. Of note, there was a distinct craniocaudal gradient in soft tissue density, with tissues in the base of the specimen appearing more dense than tissues at the cranial end. This suggests settling of contents and resin, such as may occur with an upright specimen over time.

3.2. Discrimination between mummified tissues using single and dual-energy CT parameters

Statistically significant differences were observed across 16 of the 18 pairwise comparisons performed in this study (Table 1). CT attenuation differences between soft tissue and trabecular bone were not statistically significant when imaged at 80 keV ($p = 0.14$, ns). Effective atomic number differences were not statistically significant between trabecular bone and cortical bone ($p = 0.058$).

Table 1
Median CT attenuation values at two CT energies and median effective atomic number, stratified by tissue type. IQR = interquartile range. Z(eff) = effective atomic number.

	80 keV		140 keV		Atomic number	
	(HU)	IQR	(HU)	IQR	Z(eff)	IQR
Linen	−578.3	79.4	−583.3	83.6	4.35	2.25
Soft tissue	32.2	265.1	−49.7	260.2	8.76	0.58
Trabecular bone	−69.0	197.3	−262.7	154.8	12.42	1.24
Cortical bone	374.0	427.6	180.0	266.65	11.1	1.66

3.3. Atomic number imaging offers superior contrast between soft tissue and trabecular bone when compared to single energy CT

Effective atomic number was a superior discriminator between soft tissue and trabecular bone when compared to conventional single energy imaging (Fig. 3),. Imaging at 80 keV did not reliably discriminate between soft tissue and trabecular bone ($p = 0.14$). Imaging at 140 keV did demonstrate statistically significant attenuation differences between soft tissue and trabecular bone ($p < 0.003$), however the magnitude of the contrast was smaller than that observed with effective atomic number imaging (Table 2).

3.4. Practical example of using effective atomic number imaging in paleoradiological analysis: assessment of feline cervical spine

Specimen A40437 demonstrated a cervical spine fracture with characteristics confirming it was a post mortem fracture. No evidence of a pre- or peri-mortem cervical spine fracture was seen.

In specimen A40436, the cervical spine was unable to be clearly identified on initial inspection. In the expected region of the cervical spine in the neck, there was ill-defined high CT attenuation without morphologically normal vertebral bodies. This raised the question of whether: the cervical spine had been displaced to another cavity of the specimen; had been removed completely; remains intact and in situ, but has reduced in density and been compressed over time to the point where it no longer resembles cervical vertebrae.

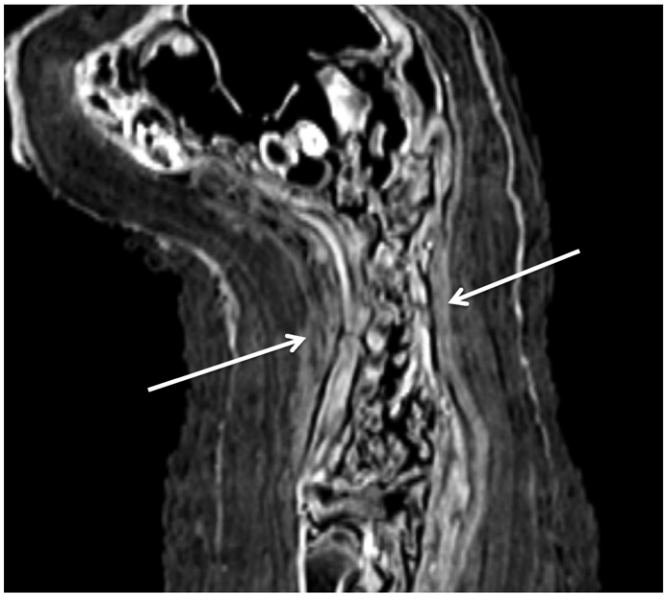

Fig. 2. Sagittal slice demonstrates a transverse fracture line through cervical spine of A40437. The fracture extends into the adjacent soft tissue planes (arrows), confirming this is a post-mortem fracture that occurred once tissues had desiccated.

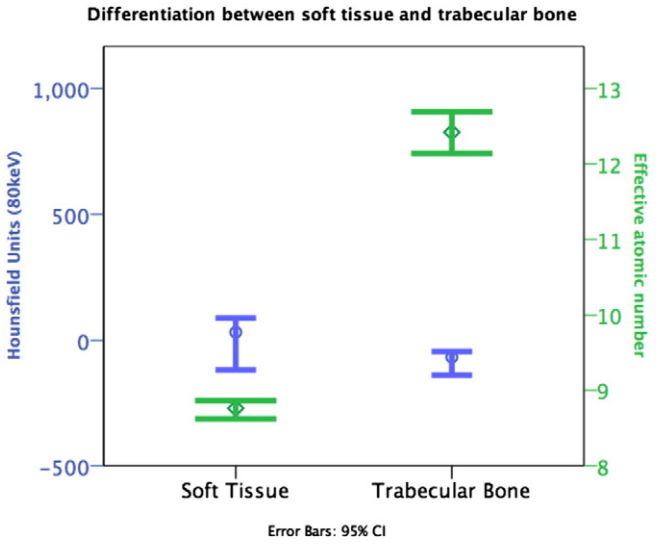

Fig. 3. Effective atomic number is a superior discriminator between soft tissue and trabecular bone, when compared with single energy imaging at 80 keV. Median attenuation values at 80 keV of each tissue type is plotted in blue and with respect to the y-axis on the left. Median effective atomic number of each tissue type is plotted in green and with respect to the y-axis on the right.

Table 2
Magnitude of the difference in values between soft tissue and trabecular bone.

	Effect size 'r'
80 keV	0.15
140 keV	0.58
Effective atomic number imaging	0.86

Calculated non-parametric effect size 'r', derived from Mann–Whitney testing. Effect size is a standardized measure used to compare tissue contrast between single energy imaging (using Hounsfield units) and effective atomic number imaging, given they use two different scales. The higher the effect size, the greater the contrast between two tissues.

Conventional CT imaging through the neck using Hounsfield units was unable to confirm or exclude the presence of bone. Hounsfield units in the area of interest were 88HU (at 80 keV) and 81HU (at 140 keV). These values fall within the interquartile range for both soft tissue and bone in our specimens (see Table 1). Analyzing the region of interest using effective atomic number demonstrates a maximum effective atomic number in this location of 8.08. Using Table 1, this value is closest to soft tissue composition, but is significantly lower than expected if the region of interest included bone. Consequently, our confidence that there are no cervical vertebrae in the cat's neck is increased.

In addition to local quantitative analysis using effective atomic number ROI markers, maps of effective atomic number can be overlaid on top of conventional greyscale CT images (Fig. 4). This method allows a more intuitive analysis of the material composition of a region. This demonstrates absence of any material in the neck of high atomic number (green or red overlay), effectively excluding bone in the region. This implies that the bony cervical spine has either displaced into another body cavity or been removed completely. A further differential is that the specimen comprises body parts from two separate cats. There is, however, no evidence of a pre- or peri-mortem cervical spine fracture.

4. Discussion

This study represents the first documented analysis of mummified remains using effective atomic number as a tissue discriminator.

Differentiating desiccated and mummified soft tissues from low-density bone is a significant problem in paleoradiology. As a specimen becomes more dehydrated, densities of soft tissues increase. This makes soft tissue more difficult to distinguish from low density bone using conventional single energy CT.

Attempts to improve differentiation using magnetic resonance imaging (MRI) are emerging (Özen et al., 2016; Rühli et al., 2007a; Shin et al., 2010) but remain necessarily limited by the extremely low levels of water in ancient specimens. MRI depends heavily on a high concentration of water molecules to produce a diagnostic image.

It is evident that imaging on the basis of density (single-energy CT) and water content (MRI) are fundamentally limited methodologies in analyzing ancient tissues. Effective atomic number imaging offers a solution to this problem as it works by imaging a material parameter that remains relatively constant over time – its elemental composition.

This study demonstrates that effective atomic number imaging can overcome the limitations posed by the effects of tissue dehydration and can differentiate mummified soft tissue from low-density bone. The results show additive benefit in performing quantitative analysis, in the form of applying region of interest markers to tissues to calculate effective atomic numbers, as well as qualitative analysis, performed by overlaying maps of effective atomic number on conventional CT images.

The absence of any statistical difference between the effective atomic number of cortical and trabecular bone, despite their grossly divergent physical densities, supports the concept that the elemental composition of mummified tissues remains relatively preserved over time, acknowledging a degree of tissue diagenesis.

A limitation of this study is that the imaged specimens contain minimal clearly identifiable embalming materials, such as pools of natron salts or resin. Discriminating mummification solutions from soft tissues and bones is a major difficulty in radiological analysis of human mummies (Rühli et al., 2004; Rühli et al., 2007b). Examination of the use of effective atomic number imaging in differentiating embalming substances from body tissue will be addressed in future research. A further limitation is the small size of the ROI markers used for different tissue types, necessitated by the small size of the mummified cat specimens. This increases statistical noise and reduces the strength of conclusions.

In addition to effective atomic number, there are a number of other unique physical properties of a specimen that can be derived using dual energy CT. Atomic number imaging was investigated in this study due to its perceived theoretical advantages. Electron density and dual energy index (DEI) are two other intrinsic material parameters able to be derived with dual energy imaging that have not been examined in the current study. Future research could examine the utility of these variables in paleoradiological research.

5. Conclusion

This study demonstrates that effective atomic number imaging can accurately differentiate desiccated soft tissues from low density bone in ancient remains. Atomic number imaging generates superior contrast between mummified bodily tissues when compared to single energy CT, improving diagnostic confidence for the paleoradiologist.

Future research will examine the efficacy of atomic number imaging in differentiating mummification solutions from bodily tissues. The diagnostic utility of other dual-energy derived material properties, such as electron density and dual energy index, remains to be investigated.

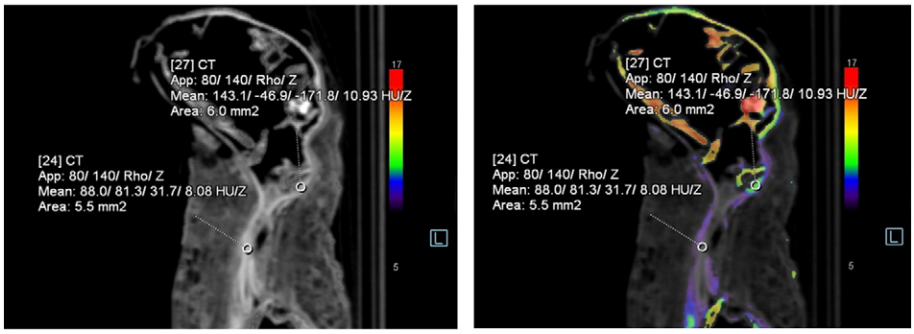

Fig. 4. On the left, region of interest markers placed over the expected location of the neck vertebrae in A40436 do not demonstrate effective atomic numbers consistent with bone. A ROI has been placed over bone in the skull base for comparison purposes. On the right, colour overlay maps show structures of high atomic number as red or green. It can be seen that there is no high atomic number tissue in the neck, adding weight to the conclusion that there are no cervical vertebrae remaining in the neck.

Conflicts of interest and funding

The authors declare that they have no conflict of interest. This research received no specific grant from any funding agency in the public, commercial or not-for-profit sectors.

Acknowledgements

The authors would like to thank Dr. Kirsten Gormley for reviewing the manuscript and Ms. Mishelle Korlaet for assistance with image reconstructions.

References

Armitage, P.L., Clutton-Brock, J., 1981. A radiological and histological investigation into the mummification of cats from ancient Egypt. J. Archaeol. Sci. 8 (2), 185–196 (Jun 30).
Brooks, R.A., 1977. A quantitative theory of the Hounsfield unit and its application to dual energy scanning. J. Comput. Assist. Tomogr. 1 (4), 487–493 (Oct 1).
Bushberg, J.T., Boone, J.M., 2011. The Essential Physics of Medical Imaging. Lippincott Williams & Wilkins (Dec 20).
Fritz, C.O., Morris, P.E., Richler, J.J., 2012. Effect size estimates: current use, calculations, and interpretation. J. Exp. Psychol. Gen. 141 (1), 2–18 (Feb).
Gostner, P., Bonelli, M., Pernter, P., Graefen, A., Zink, A., 2013. New radiological approach for analysis and identification of foreign objects in ancient and historic mummies. J. Archaeol. Sci. 40 (2), 1003–1011 (Feb 28).
Ikram, S. (Ed.), 2005. Divine Creatures: Animal Mummies in Ancient Egypt. American University in Cairo Press.
Ikram, S., Slabbert, R., Cornelius, I., du Plessis, A., Swanepoel, L.C., Weber, H., 2015. Fatal force-feeding or gluttonous gagging? The death of kestrel SACHM 2575. J. Archaeol. Sci. 63, 72–77 (Nov 30).
Johnson, T.R., Krauss, B., Sedlmair, M., Grasruck, M., Bruder, H., Morhard, D., Fink, C., Weckbach, S., Lenhard, M., Schmidt, B., Flohr, T., 2007. Material differentiation by dual energy CT: initial experience. Eur. Radiol. 17 (6), 1510–1517 (Jun 1).
McCollough, C.H., Leng, S., Yu, L., Fletcher, J.G., 2015. Dual-and multi-energy CT: principles, technical approaches, and clinical applications. Radiology 276 (3), 637–653 (Aug 24).
McKnight, L.M., Atherton-Woolham, S.D., Adams, J.E., 2015. Imaging of ancient Egyptian animal mummies. Radiographics 35 (7), 2108–2120 (Nov 12).
Özen, A.C., Ludwig, U., Öhrström, L.M., Rühli, F.J., Bock, M., 2016. Comparison of ultrashort echo time sequences for MRI of an ancient mummified human hand. Magn. Reson. Med. 75 (2), 701–708 (Feb).
Rühli, F.J., Chhem, R.K., Böni, T., 2004. Diagnostic paleoradiology of mummified tissue: interpretation and pitfalls. Can. Assoc. Radiol. J. 55 (4), 218–227 (Oct 1).
Rühli, F.J., Böni, T., Perlo, J., Casanova, F., Baias, M., Egarter, E., Blümich, B., 2007a. Non-invasive spatial tissue discrimination in ancient mummies and bones in situ by portable nuclear magnetic resonance. J. Cult. Herit. 8 (3), 257–263 (Sep 30).
Rühli, F.J., von Waldburg, H., Nielles-Vallespin, S., Böni, T., Speier, P., 2007b. Clinical magnetic resonance imaging of ancient dry human mummies without rehydration. JAMA 298 (22), 2618–2620 (Dec 12).
Shin, D.H., Lee, I.S., Kim, M.J., Oh, C.S., Park, J.B., Bok, G.D., Yoo, D.S., 2010. Magnetic resonance imaging performed on a hydrated mummy of medieval Korea. J. Anat. 216 (3), 329–334 (Mar 1).
Wade, A.D., Ikram, S., Conlogue, G., Beckett, R., Nelson, A.J., Colten, R., Lawson, B., Tampieri, D., 2012. Foodstuff placement in ibis mummies and the role of viscera in embalming. J. Archaeol. Sci. 39 (5), 1642–1647 (May 31).
Wanek, J., Székely, G., Rühli, F., 2011. X-ray absorption-based imaging and its limitations in the differentiation of ancient mummified tissue. Skelet. Radiol. 40 (5), 595–601 (May 1).